Orbital effects of strong magnetic field on a two-dimensional Holstein polaron

Subhasree Pradhan,[1,*] Monodeep Chakraborty,[1,†] and A. Taraphder[1,2,‡]
[1]*Department of Physics, Indian Institute of Technology Kharagpur, Kharagpur - 721302, India*
[2]*Center for Theoretical Studies, Indian Institute of Technology Kharagpur, Kharagpur - 721302, India*
(Received 8 July 2015; revised manuscript received 8 December 2015; published 3 March 2016)

We investigate the orbital effects of a strong external magnetic field on the ground-state properties of a two-dimensional (2D) Holstein polaron, employing variational approaches based on exact diagonalization. From the ground-state energy and the wave function, we calculate the electron-phonon correlation function, the average phonon number, and the Drude weight and investigate the evolution of a 2D Holstein polaron as a function of the magnetic flux. Although the external magnetic field affects the polaron throughout the parameter regime, we show that the magnetic field has a stronger effect on a loosely bound (spatially extended) polaron. We also find that the magnetic field can be used as a tuning parameter, particularly for a weakly coupled polaron, to reduce the spatial extent of a large polaron.

DOI: 10.1103/PhysRevB.93.115109

I. INTRODUCTION

The interplay between electronic and lattice degrees of freedom is central to many areas of condensed-matter physics. The Holstein model [1,2], which is almost seven decades old, still holds a place of eminence when it comes to electron-phonon (el-ph) interaction because of the intricate many-body physics it encompasses within a simple paradigm. On the other hand, modification of the electronic band structure on a lattice in the presence of strong magnetic field gives rise to the well-known Hofstadter's butterfly [3], a quintessential example of fractals in quantum mechanical systems. Although the physics of solids is replete with electron-phonon coupled systems, precious little is known about the effects of a strong orbital magnetic field on such a coupled system, where indeed only one of the partners, the electron, feels the effect of the field directly.

In this paper, we study the Holstein polaron in a strong magnetic field, which marries the two issues above. In the presence of strong el-ph coupling, the electron is expected to form polaronic bound states of varying size, depending on the strength of the el-ph interaction. On the other hand, an orbital magnetic field induces a precession of an electron away in an orbit reducing the net mobility, in effect subjecting it further to localization by phonons. It is in this context that the combined effect is an interesting puzzle calling for a resolution. However, the subject of lattice polarons in a strong magnetic field is largely an unexplored area, barring very few works, notably by Berciu [4] using the momentum-average (MA) approximation [5]. In the presence of a weak magnetic field, perturbative calculations with the Fröhlich-based continuum model predict that the cyclotron frequency is defined in terms of polaron effective mass [6]. Nonperturbative calculation on a two-dimensional (2D) lattice by Berciu [4] confirms these results for a very weak field and lower-lying Landau levels. Our exact-diagonalization-based numerical results at these regimes substantiate the earlier findings.

Several numerical approaches have been employed to study the Holstein model, such as density-matrix renormalization group (DMRG) techniques [7], exact-diagonalization techniques [8], the quantum Monte Carlo method [9], the global-local method [10], and advanced variational techniques [11]. The variational approaches based on the exact diagonalization (VAED) used by Bonča *et al.* [12] and Chakraborty *et al.* [13] are some of the most successful numerical methods to study the Holstein and extended-Holstein type of el-ph systems in a dilute regime in all dimensions. In this work, we have generalized this method to deal with cases where the lattice unit cell has more than one equivalent site, i.e., a supercell VAED. This scheme has been quite successfully implemented in the present case and can be used in many important situations where a many-atom unit cell is coupled to another degree of freedom (such as polarons in graphene or a case of partial disorder). We first compare our supercell-VAED zero-field results with the benchmark results available in the literature, where we find at least an eight-digit match. Then we proceed to study the ground-state Hofstadter band at different parameters of the Holstein model. We first create a variational space by repeated action of the Hamiltonian on the initial state and then we adopt a twofold approach: (i) integrate the spectral function obtained from the k-space Green's function over the Brillouin zone to get the density of states, and (ii) find the ground-state energy and wave function by employing the conjugate gradient technique [14].

This paper is organized as follows: in Sec. II, we discuss the Hamiltonian and delineate the basis generation procedures. We then proceed to show our results and compare some of those with the existing results in Sec. III. In this section, we also study the evolution of the polaron with magnetic flux in different parameter regimes and try to analyze the interplay between the el-ph interaction and the magnetic field. The conclusion follows in Sec. IV.

II. THE MODEL

In order to study the effect of the magnetic field, we employ the simplest and well-studied model for electron-phonon interaction, i.e., the Holstein model, where a spinless electron is coupled to a dispersionless optical phonon, represented by a

*spradhan@phy.iitkgp.ernet.in
†bandemataram@gmail.com
‡arghya@phy.iitkgp.ernet.in

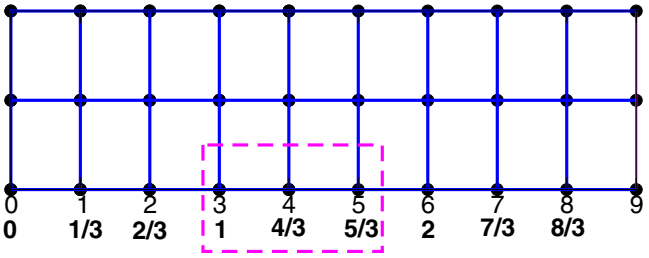

FIG. 1. The magnetic supercell (marked by the purple box) for a magnetic field of $\frac{2\pi}{3}$. The figure shows the variation in hopping phases along the y bonds due to the choice of Landau gauge.

local Einstein oscillator. For a spinful model, the magnetic field leads to the Zeeman splitting of up- and down-spin polaron bands. In a very high magnetic field and low electron density, one can consider only orbital effects and ignore the Zeeman splitting as the Hilbert space is spin split into two sectors well separated in energy. One can, therefore, concentrate on the lower of the two for low filling, effectively reducing the model to a spinless one. The Hamiltonian is given by

$$H = -\sum_{i,j} t_{ij}(c_i^\dagger c_j + \text{H.c.}) + \omega \sum_i b_i^\dagger b_i - \omega g \sum_i c_i^\dagger c_i (b_i^\dagger + b_i), \quad (1)$$

where $\langle i,j\rangle$ are nearest-neighbor site indices on a square lattice, and c_i (b_i) are electron (phonon) annihilation operators, respectively. The nearest-neighbor hopping integral in the presence of a magnetic field is now associated with a Peierls phase factor. The choice of Landau gauge $\vec{A}(r) = B(0,ma,0)$ for a uniform magnetic field B perpendicular to the plane of the lattice leads to the hopping integral $t_{ij} = -t$ along the x direction, and $t_{ij} = -te^{ie/\hbar \int_j^i A(\vec{r})d\vec{r}} = -t\exp(\pm 2\pi i m \frac{\phi}{\phi_0}) = -t\exp(\pm 2\pi i m \frac{p}{q})$ along the y direction. m denotes the x component of the lattice position vector. Here, $\phi = Ba^2$ is the number of flux quanta per plaquette, which is the gain of phase by an electron hopping around a closed path along the plaquette. Here, a indicates the lattice parameter, taken to be one throughout. $\frac{\phi}{\phi_0} = \Phi = \frac{p}{q}$, with p, q the co-prime integers and ϕ_0 the Dirac flux quantum. We have set the hopping integral t to be 1 throughout the numerical calculation and all other parameters are defined in units of t. Here, ω is the oscillator frequency and g is the dimensionless electron-phonon coupling strength. The effect of electron-phonon coupling is expressed in terms of the dimensionless parameter g.

Once the magnetic field is switched on, we lose lattice periodicity in the x direction. However, since it is only a phase repeating at every 2π, periodicity is still retained, albeit with a changed value. Figure 1 describes the situation for a magnetic field $B = \frac{2\pi}{3}$. In this case, the changed periodicity of the lattice is 3; so instead of the one-site unit cell, our magnetic unit cell is basically a three-site strip. Therefore, to account for a magnetic field $B = \frac{2\pi}{N}$, the magnetic supercell will be a strip of length N, so that the variation in hopping phases along the y bonds is accounted for. The variational basis is similar to that of Bonča *et al.* [12]. The difference is that now instead of one initial zero-phonon state, we start with N zero-phonon states (for N different positions of the magnetic strip) and, while checking for the translational symmetry, we shift the supercell. Mathematically, this amounts to putting another index m to account for the position-dependent parameter. For example, if $\phi = 0.005$, which corresponds to $N = 200$, the size of the supercell will be 200. Therefore, initially we will have 200 starting states, i.e., an electron present at one of the inequivalent sites of the supercell. When the Hamiltonian is acted on these initial states, retaining the translational symmetry, 200 more states are generated with a phonon present at the site of the electron. It is important to note that since translational symmetry is taken care of, if a basis state can be generated in more than one way, only one copy is retained [12]. Hence this method is exactly the same as the VAED method of Bonča *et al.* [12], except that we have an extended unit cell (supercell) with more than one site to accommodate the inequivalent hopping phases due to the magnetic field. Therefore, if the Hamiltonian is operated, say, N_h times (N_h shells), we will have states with N_h phonon quanta at the electron site and no phonon excitations elsewhere. There will also be states with $N_h - 1$ phonon quanta at the adjacent site of the electron with no phonon elsewhere. Further, N_h times operation of the Hamiltonian will ensure that we have states with at least one phonon excitation at a site that is $N_h - 1$ sites away from the electron. This method of basis construction ensures an accurate basis for a spatially large polaron and for polarons at the intermediate-coupling regime. However, the basis required for a small polaron at strong el-ph coupling is very different. For a strongly coupled small polaron, we know from Lang-Firsov theory that all types of phonon excitation are required at the electron site. In order to get a converged basis for a small polaron ($\omega = 5$ and $g = 2$), we have appropriated the idea of Lang-Firsov transformation while constructing the basis [13,15]. This method enhances the numerical accuracy for the small polarons as has been established by earlier works, since it incorporates into the basis the important states which a small polaron requires [13,15].

The numerical accuracy of a particular calculation for a given set of parameters is determined by comparing the results (the ground-state energy and the correlation functions calculated from the ground-state wave function) obtained from a basis of N_h shells with that of the results from a basis of $N_h - 1$ shells. Similarly for the density of states (DOS), we compare the DOS calculated from a particular shell with its previous shell. The supercell VAED implemented in this work ensures an accuracy of 6–8 decimal places for the calculated ground-state energies and at least an accuracy of 3–4 decimal places in the correlation functions for all of the calculated regimes. An excellent match of the DOS for the low-lying states is also obtained. In order to check the accuracy of our method, we have considered the sum rules for the spectral weight $A(\boldsymbol{k},\omega) = -\frac{1}{\pi}\text{Im}G(\boldsymbol{k},\omega)$, defined as [5,16]

$$M_n(\boldsymbol{k}) = \int_{-\infty}^{\infty} d\omega \omega^n A(\boldsymbol{k},\omega). \quad (2)$$

For a singly dressed particle such as a polaron, the sum rules can be evaluated up to an arbitrary order and can be rewritten

in a simplified way [5],

$$M_n(\boldsymbol{k}) = \langle 0|c_{\boldsymbol{k}} H^n c_{\boldsymbol{k}}^\dagger|0\rangle. \tag{3}$$

We have obtained the first five vacuum expectation values and they are [5,16]

$M_0(\boldsymbol{k}) = 1$, $M_1(\boldsymbol{k}) = \epsilon_{\boldsymbol{k}}$, $M_2(\boldsymbol{k}) = \epsilon_{\boldsymbol{k}}^2 + (g\omega)^2$, $M_3(\boldsymbol{k}) = \epsilon_{\boldsymbol{k}}^3 + 2(g\omega)^2\epsilon_{\boldsymbol{k}} + g^2\omega^3$, and $M_4(\boldsymbol{k}) = \epsilon_{\boldsymbol{k}}^4 + (g\omega)^2[3\epsilon_{\boldsymbol{k}}^2 + 2dt^2] + 2g^2\omega^3\epsilon_{\boldsymbol{k}} + [g^2\omega^4 + 3(g\omega)^4]$, where d denotes the dimension of the lattice and t the hopping integral. We have verified the first five sum rules for a 1D and 2D Holstein model at different el-ph regimes and $\boldsymbol{k}$ values, and our calculated values are at least 99.5% of the exact values. For a 1D Holstein model, they also match excellently with those obtained from MA calculations. We have also tested the sum rules for the supercell calculation at $B = 0$ and we find a similar matching. It is worth mentioning that $M_4(\boldsymbol{k})$ is the first moment which involves the dimensionality of the lattice other than the bare energy $\epsilon_{\boldsymbol{k}}$ [16].

We calculate the following quantities of interest: To calculate the correlation between the electron position and the lattice distortion in the ground state, we define a correlation function $\chi(\vec{r})$ [$\chi(x,y)$] as follows:

$$\chi(\vec{r}) = \langle \Psi_G|c_i^\dagger c_i(b_{i+\vec{r}}^\dagger + b_{i+\vec{r}})|\Psi_G\rangle, \tag{4}$$

where ψ_G is the ground-state wave function. The total lattice deformation is conserved to $2g$ in the Hamiltonian, from a straightforward sum rule. The average phonon number is calculated as

$$N^{ph} = \sum_i \langle \psi_G|{b_i}^\dagger b_i|\psi_G\rangle. \tag{5}$$

The distribution of the number of phonons in the vicinity of the electron is given by

$$\gamma(\vec{r}) = \langle \Psi_G|c_i^\dagger c_i(b_{i+\vec{r}}^\dagger b_{i+\vec{r}})|\Psi_G\rangle. \tag{6}$$

The Drude weight (D_0) of the ground state of the polaron is obtained by introducing a phase factor isotropically to the hopping matrix elements ($t \to te^{i\eta}$) and then finding out the response to the electric current as

$$D_0 = \left.\frac{\partial^2 E_0(\eta)}{\partial \eta^2}\right|_{\eta=0}, \tag{7}$$

where $E_0(\eta)$ is the eigenenergy of the ground state in the presence of nonzero η [13]. The calculated D_0 has been normalized with respect to a free electron on a square lattice for all cases.

III. RESULTS

We first test the numerical accuracy of our result by comparing the ground-state energy of a Holstein polaron at $\omega = 2$ and $g = 1$ with the best available results in the literature [12,13]. The ground-state energy for this parameter is $-4.814\,735\,77$, obtained from a variational basis constructed by operating the Hamiltonian 11 times on the initial states ($N_h = 11$) [12], which matches up to eight decimal places with the result of Bonča *et al.* [12]. Then we compare our calculated density of states (DOS) both for a free electron on a lattice and polaron with those obtained by Berciu [4]. Figure 2 displays

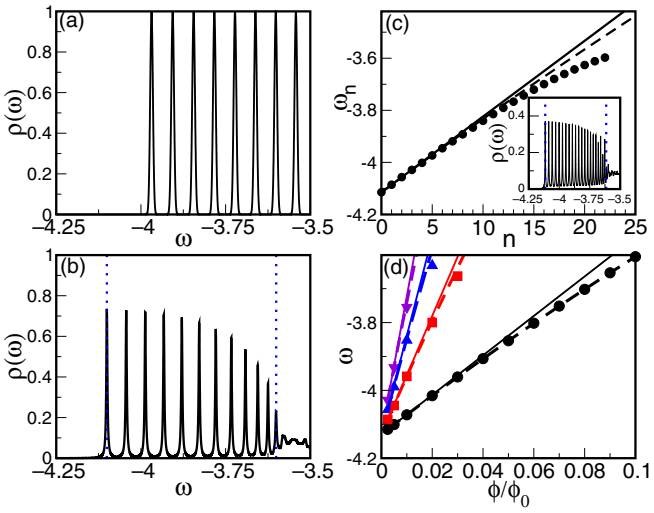

FIG. 2. (a) The lower-lying Landau levels for an electron in a lattice; (b) the same for a Holstein polaron calculated at $\omega = 0.5$ and $g = \sqrt{0}.4$. The dashed vertical lines mark the ground-state energy at E_0 and $E_0 + \omega$. (c) Energies ω_n of the Landau levels vs n for $\phi = 0.0025$. The solid lines are the perturbational prediction with our calculated effective mass and the dashed lines are with $m^*(B) = m^*(1 + \gamma B)$. The inset shows the Landau levels at $\phi = 0.0025$, where the dashed vertical line denotes the same as in (b). (d) The energy of the four lowest Landau levels as a function of ϕ for $\lambda = 0.2$ ($\lambda = \frac{g^2\omega}{4t}$). The circles, squares, upper triangles, and lower triangles denote the first, second, third, and fourth Landau levels, respectively. The solid and dashed lines have the same significance as (c).

the Landau levels for a magnetic flux (ϕ) of strength 0.005, for an electron [Fig. 2(a)] and that of a polaron [Fig. 2(b)] at $\omega = 0.5$ and $g = \sqrt{0}.4$ (corresponding to $\lambda = 0.2$ of Berciu [4] where $\lambda = \frac{g^2\omega}{4t}$). In order to accommodate a flux of value 0.005, the size of our magnetic supercell (or magnetic strip) had to be 200 with $N_h = 9$.

The vertical dotted lines of Fig. 2(b) indicate the ground-state energy E_0 and $E_0 + \omega$, respectively. The distinct polaron Landau levels lose their identity beyond $E_0 + \omega$. We digress a bit and compare the scenario of an electron in a lattice with that of a Holstein polaron without bringing the magnetic field into consideration. The electron has only a single band, whereas a Holstein polaron has an infinite number of bands as the electron is coupled to all possible phononic excitations. However, for a Holstein polaron, we have a gap of ω at $k = 0$ in between the ground state and the first excited state; beyond that we have a huge number of closely spaced states (depending on the parameter regime) and as we go up in energy they acquire a quasicontinuum nature. These are the states that disturb the sharpness of the Landau levels beyond $E_0 + \omega$ in Fig. 2(b). The point that merits mention is that the first excited state of the Holstein polaron at $k = 0$ consists of the ground-state polaron and an excited phonon. The excited phonon wants to be infinitely away from the ground-state polaron; therefore the larger the variational space (N_h), the more accurate will be the first excited state. Ideally, the first excited state can be exact only in the thermodynamic limit. Hence the accuracy of the variational space based calculation in the vicinity and above $E_0 + \omega$ will be a function of

N_h. We now compare our calculated results with those of the perturbative calculation based on the continuum model. Figure 2(c) shows the energies ω_n as a function of the levels n for $\phi = 0.0025$. The perturbative calculation gives the energy levels as

$$\hbar\omega_n = E_{GS} + \hbar\omega_c^*\left(n + \tfrac{1}{2}\right), \tag{8}$$

where $\omega_c^* = \frac{eB}{m^*}$ is the cyclotron frequency and we have taken the $B = 0$ value of the polaron effective mass m^* and E_{GS} from our numerical results ($E_{GS} = -4.129607$ and $\frac{m^*}{m} = 1.079$). In Fig. 2(c), the solid line is calculated using Eq. (8) and its disagreement with our calculated energies with increasing n is clearly visible. The perturbation theory [4,6] gives a correction to the polaron effective mass as a function of the field B [$m^*(B) = m^*(1 + \gamma B)$, where γ is a function of n]. When we substitute $m^*(B)$ in place of the polaron mass at $B = 0$ in Eq. (8) (the dashed lines), we get a better agreement with our calculated results; however, disagreement reappears with further increase in n (as we reach the vicinity of $E_0 + \omega$). Figure 2(d) shows the first four calculated Landau levels as a function of ϕ and compares them with the perturbative results using the polaron mass and field-corrected polaron mass (solid line and dashed line, respectively). The perturbative results with field-corrected polaron effective mass are in excellent agreement with the lowest calculated Landau levels for all shown field values. However, with increasing n and B, the supercell (SC)-VAED calculated results start to differ from the perturbative calculations. Here our calculated results and conclusions are in agreement with the nonperturbative MA results of Berciu [4].

We now investigate the response of the polaron to magnetic fields. The average phonon number (N_{ph}) gives an idea about the phononic activity of the polaron. An increase in the value of N_{ph} suggests an increase in the phononic attributes of the polaron. Figure 3(a) shows the variation (relative to the zero-field value) of N_{ph} at three different regimes. At $\omega = 1$ and $g = 0.05$, we have a quasifree electron at $B = 0$, and the phonon activity clearly increases with the increase in field values, achieving a maximum in the vicinity of $\phi = 0.375$. Though the trend is similar at $\omega = 2$ and $g = 1$, the relative variation is much less pronounced. At $\omega = 5$ and $g = 2$, we are deep in the antiadiabatic limit ($\omega \gg t$), and polarons of small spatial extent hardly respond to the variation in magnetic field. Figure 3(b) shows the relative variation (with respect to the zero-field value) of ground-state energy with field for the same set of el-ph parameters. The pattern in ground-state energy variation is the same for all three parameter regimes and one can recognize them as the ground-state Hofstadter band. The relative change is again maximum for a weakly bound polaron and minimum for the polaron in the antiadiabatic limit; the signature of the magnetic field shows up in the ground-state energy pattern for all regimes. The variation in average phonon number as well as ground-state energy with applied magnetic flux follows the lowest branch of the Hofstadter butterfly. Both Figs. 3(a) and 3(b) are symmetric about $\phi = 0.5$, which are typical Hofstadter characteristics. The maximum size of the magnetic strip used for this calculation is 64 and all strip sizes lower than 64 are included in the figure. The basis size $N_h = 10$ has been used for $\omega = 1$ and $g = 0.05$ as well as for the $\omega = 2$ and $g = 1$ case. Therefore, the maximum number of phonons that a state can have is 10. The $\omega = 5$ and $g = 2$ calculation has been performed, taking into consideration the Lang-Firsov ideas with $N_h = 7$. Consequently, the maximum number of phonons that a state can have is 27, as initially the starting basis contains phonon excitations up to 20 at the electron site.

A thorough study of the electron-lattice correlation functions throws some light on the mechanism of increased phononic activity for a weakly bound polaron and a much smaller effect in the antiadiabatic regime. A strip size of 16 has been used to calculate this correlation function. Figure 4 shows the $\chi(x,y)$ for four different values of ϕ ($\phi = 0.0, 0.1875, 0.375$, and 0.5) for a polaron at $\omega = 1$ and $g = 0.05$. The displayed $\chi(x,y)$ has been divided by the total deformation $2g$ for convenience. Though the total lattice distortion of the polaron always adds up to $2g$, it can be seen that χ increases locally. The local distortion assumes a higher value for $\chi(x,y) = \chi(0,0)$ and also in its vicinity

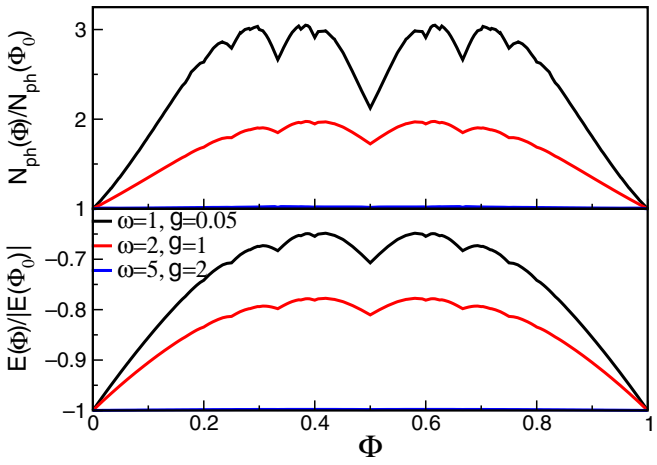

FIG. 3. Upper panel: The average phonon number N_{ph} as a function of magnetic field for three different sets of el-ph coupling; N_{ph} are normalized by their respective zero-field values. Lower panel: The ground-state energy E_0 (normalized by their respective zero-field values) as a function of magnetic field for three sets of el-ph coupling.

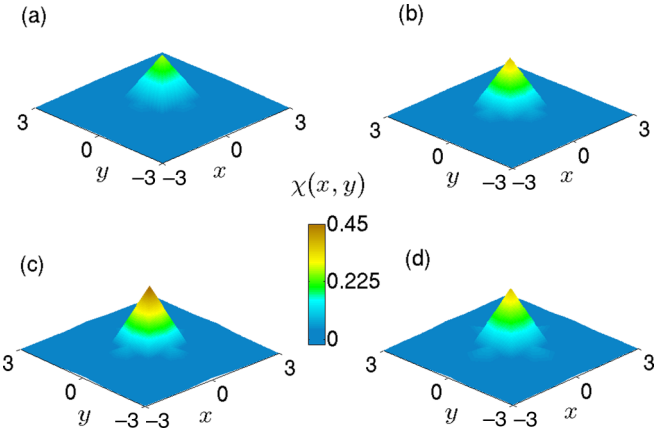

FIG. 4. The electron-lattice correlation function $\chi(x,y)$ measures the lattice distortion, shown at four different magnetic flux values. The el-ph parameter for the polaron is $\omega = 1$ and $g = 0.05$.

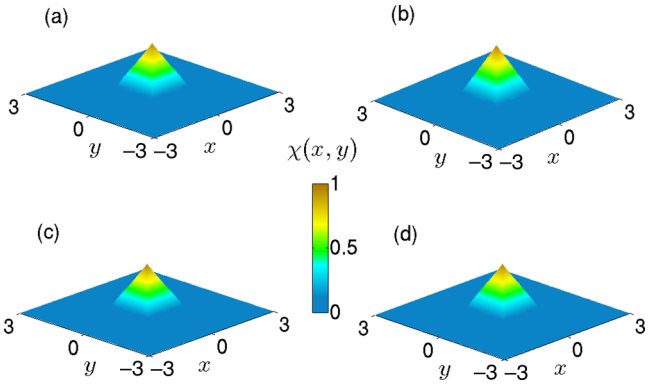

FIG. 5. The electron-lattice correlation function $\chi(x,y)$ at four different magnetic flux values. The respective parameters are $\omega = 5$ and $g = 2$.

than farther outside, i.e., we have a relatively tightly bound polaron (as compared to the $\phi = 0$ polaron). The $\chi(0,0)$ for $\phi = 0$ is 0.025 and reaches a maximum at $\phi = 0.375$ to 0.043. A similar trend is observed for $\gamma(x,y)$ as well. Figure 5 shows the electron-lattice correlation at the same four values of ϕ ($\phi = 0.0, 0.1875, 0.375$, and 0.5) for a polaron in the antiadiabatic regime ($\omega = 5$ and $g = 2$). An extremely small polaron results in this regime and, as it is quite evident, almost the entire distortion is rooted at $(x,y) = (0,0)$; there is no noticeable change with magnetic field. The $\chi(0,0)$ for $\phi = 0$ is 3.90 and reaches a maximum at $\phi = 0.375$ to 3.943, a very small change. A study of Figs. 4 and 5 clearly shows that the magnetic field brings about a prominent change in a weakly bound polaron compared to a polaron that is tightly bound to the lattice. The magnetic field tends to shrink the distortion towards its center for a weakly bound polaron, whereas it can hardly affect a strongly bound one. Clearly, a loosely bound polaron has a much larger orbit and therefore has a stronger effect due to the orbital magnetic field. Hence, we see in Fig. 4 the relative increase in $\chi(0,0)$, though the sum total of distortion is limited to $2g$ (as expected from the sum rule).

The Drude weight (D_0) gives the measure of coherence and is an important correlation function to study the nature of electronic conductivity of a system. There have been a number of earlier works suggesting a magnetic-field-induced metal-insulator transition [17]. The Drude weight is calculated [Eq. (7)] by introducing a global phase in hopping along the x and y direction isotropically. Figure 6 shows the calculated D_0 as a function of field for the three el-ph regimes. The size of the magnetic strip used for this calculation is 16. At $\omega = 1$ and $g = 0.05$, we have a quasifree electron very weakly tied to the lattice, with a large spatial extent. Consequently, at $\phi = 0$, $D_0 \approx 1$. However, for small magnetic flux ($\phi = \frac{1}{16}$), it almost drops to 0, suggesting a complete loss of coherent hopping. Figures 6(a)–6(c) show the ground-state band for five different flux values ($\phi = 0.0$, $\frac{1}{16}$, $\frac{1}{4}$, $\frac{3}{8}$, and $\frac{1}{2}$) for three different el-ph regimes. At $\phi = \frac{1}{16}$, it shows a completely flat band (within the numerical accuracy of our calculation) and $\frac{dE_k}{dk} = 0$ throughout the Brillouin zone, which arises from local quantum interferences [18]. The electron, while moving through the lattice, will see a maximum variation in flux for the smallest value of field and loses its coherence. However, the ground-state band is not completely flat, and for $\phi = \frac{1}{4}, \frac{3}{8}, \frac{1}{2}$

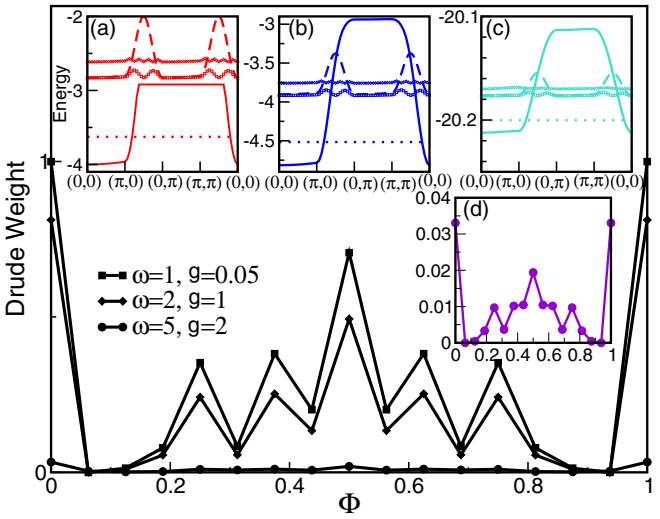

FIG. 6. Drude weight D_0 (normalized by the free electron D_0) vs magnetic flux. Insets (a)–(c) shows the ground-state band at $\phi = 0.0$ (solid line), $\phi = \frac{1}{16}$ (dotted line), $\phi = \frac{1}{4}$ (open square), $\phi = \frac{3}{8}$ (open diamond), and $\phi = \frac{1}{2}$ (dashed line) for ($\omega = 1$, $g = 0.05$), ($\omega = 2$, $g = 1$), and ($\omega = 5$, $g = 2$), respectively. Inset (d) shows D_0 for $\omega = 5$ and $g = 2$ separately.

etc., we find peaks in D_0. Though the present calculation has been shown with a magnetic strip size of 16, this argument is valid for any strip size and complete loss of coherence can be observed at $\phi = \frac{1}{N}$, for a magnetic strip size of N. The D_0 peaks for $\omega = 2$ and $g = 1$ have slightly reduced values as we are in the intermediate el-ph coupling regime and no longer have the quasifree electron. For the $\omega = 5$ and $g = 2$ antiadiabatic strong-coupling regime, the exponential suppression of the D_0 is observed. However, the change in magnetic flux still has its influence, which can be seen in Fig. 6(d), and local quantum interferences show up its effect at the smallest magnetic flux ($\phi = \frac{1}{16}$). This phenomenon leads to the localization and consequent vanishing of D_0. Clearly, in the antiadiabatic limit, the more localized the carrier gets, the Lorentz force is less likely to affect the dynamics. The quantum interference effects become more pronounced in this phonon-assisted hopping regime, as borne out in Fig. 6. A similar observation has been made by Böttger *et al.* [19] in the context of the influence of the magnetic field on transport in small polarons. We see a magnetic-field-induced coherent to incoherent transition at $\phi = \frac{1}{16}$ across the el-ph coupling regime for a lattice size of 16.

IV. SUMMARY AND CONCLUSION

We have developed a numerical scheme based on VAED to study the el-ph interaction in the presence of a strong magnetic field. Our results are in excellent agreement with earlier results wherever a comparison is possible. The external magnetic field changes the orbit of motion of the electron and the effect is more in the case of loosely bound polaron already spread out in real space. With the inclusion of the magnetic field, we see that the spatial extent of the polaron decreases, resulting in a polaron with a tighter binding. Our method can be useful to many important cases with a more complex unit cell.

ACKNOWLEDGMENTS

We thank Mona Berciu for sharing her MA results. We gratefully acknowledge Narayan Mohanta and Sugata Pratik Khastgir for useful and stimulating discussion. We acknowledge the use of the computing facility from the DST-Fund for Improvement of S&T infrastructure (phase-II) Project installed in the Department of Physics, IIT Kharagpur, India.

[1] T. Holstein, Ann. Phys. (NY) **8**, 325 (1959).

[2] For a review, see H. Fehske and S. A. Trugman, in *Polarons in Advanced Materials*, edited by A. S. Alexandrov (Springer-Verlag, Dordrecht, 2007).

[3] D. R. Hofstadter, Phys. Rev. B **14**, 2239 (1976).

[4] M. Berciu, Phys. Rev. B **82**, 201102(R) (2010).

[5] M. Berciu, Phys. Rev. Lett. **97**, 036402 (2006); G. L. Goodvin, M. Berciu, and G. A. Sawatzky, Phys. Rev. B **74**, 245104 (2006); M. Berciu and G. L. Goodvin, *ibid.* **76**, 165109 (2007); G. L. Goodvin and M. Berciu, *ibid.* **78**, 235120 (2008); L. Covaci and M. Berciu, Phys. Rev. Lett. **102**, 186403 (2009); M. Berciu and H. Fehske, Phys. Rev. B **82**, 085116 (2010).

[6] S. Das Sarma, Phys. Rev. Lett. **52**, 859 (1984); R. Chen, D. L. Lin, and T. F. George, Phys. Rev. B **41**, 1435 (1990); F. M. Peeters, X. G. Wu, J. T. Devreese, C. J. G. M. Langerak, J. Singleton, D. J. Barnes, and R. J. Nicholas, *ibid.* **45**, 4296 (1992); G. Q. Hai, F. M. Peeters, and J. T. Devreese, *ibid.* **47**, 10358 (1993); D. E. N. Brancus and G. Stan, *ibid.* **63**, 235203 (2001); Y. Chen, N. Regnault, R. Ferreira, B. F. Zhu, and G. Bastard, *ibid.* **79**, 235314 (2009).

[7] E. Jeckelmann and S. R. White, Phys. Rev. B **57**, 6376 (1998).

[8] A. S. Alexandrov, V. V. Kabanov, and D. K. Ray, Phys. Rev. B **49**, 9915 (1994); G. Wellein, H. Roder, and H. Fehske, *ibid.* **53**, 9666 (1996); G. Wellein and H. Fehske, *ibid.* **56**, 4513 (1997); **58**, 6802 (1998); E. V. L. de Mello and J. Ranninger, *ibid.* **55**, 14872 (1997); M. Capone, W. Stephan, and M. Grilli, *ibid.* **56**, 4484 (1997); F. Marsiglio, Physica C **244**, 21 (1995).

[9] H. De Raedt and A. Lagendijk, Phys. Rev. Lett. **49**, 1522 (1982); Phys. Rev. B **27**, 6097 (1983); **30**, 1671 (1984); P. E. Kornilovitch and E. R. Pike, *ibid.* **55**, R8634(R) (1997); J. P. Hague, P. E. Kornilovitch, A. S. Alexandrov, and J. H. Samson, *ibid.* **73**, 054303 (2006); A. S. Mishchenko, N. Nagaosa, G. De Filippis, A. de Candia, and V. Cataudella, Phys. Rev. Lett. **114**, 146401 (2015).

[10] A. W. Romero, D. W. Brown, and K. Lindenberg, J. Chem. Phys. **109**, 6540 (1998).

[11] G. De Filippis, V. Cataudella, G. Iadonisi, V. Marigliano Ramaglia, C. A. Perroni, and F. Ventriglia, Phys. Rev. B **64**, 155105 (2001).

[12] J. Bonča, S. A. Trugman, and I. Batistic, Phys. Rev. B **60**, 1633 (1999); J. Bonča, T. Katrasnik, and S. A. Trugman, Phys. Rev. Lett. **84**, 3153 (2000); L. C. Ku, S. A. Trugman, and J. Bonča, Phys. Rev. B **65**, 174306 (2002); J. Bonča and S. A. Trugman, *ibid.* **64**, 094507 (2001).

[13] A. Chakrabarti, M. Chakraborty, and A. Mookerjee, Physica B **388**, 63 (2007); M. Chakraborty, A. N. Das, and A. Chakrabarti, J. Phys.: Condens. Matter **23**, 025601 (2011); M. Chakraborty, B. I. Min, A. Chakrabarti, and A. N. Das, Phys. Rev. B **85**, 245127 (2012); M. Chakraborty and B. I. Min, *ibid.* **88**, 024302 (2013); M. Chakraborty, M. Tezuka, and B. I. Min, *ibid.* **89**, 035146 (2014).

[14] V. S. Viswanath and G. Müller, *The User Friendly Recursion Method: a Cookbook for Eclecticists, Troisieme Cycle de la Physique, En Suisse Romande* (M. D. Reymond, Université de Lausanne, 1991).

[15] Z. Li, D. Baillie, C. Blois, and F. Marsiglio, Phys. Rev. B **81**, 115114 (2010).

[16] P. E. Kornilovitch, Europhys. Lett. **59**, 735 (2002).

[17] J. An, C. D. Gong, and H. Q. Lin, Phys. Rev. B **63**, 174434 (2001).

[18] W. Hausler, Phys. Rev. B **91**, 041102(R) (2015).

[19] H. Böttger, V. V. Bryksin, and T. Damker, in *Polarons in Advanced Materials*, edited by A. S. Alexandrov (Canopus/Springer, Bristol, 2007); H. Böttger, V. V. Bryksin, and F. Schulz, Phys. Rev. B **48**, 161 (1993).